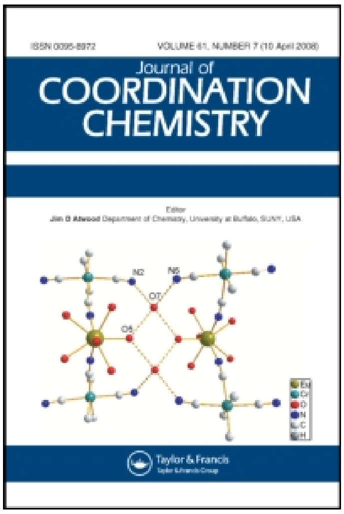

Journal of Coordination Chemistry
Publication details, including instructions for authors and subscription information:
http://www.informaworld.com/smpp/title~content=t713455674

Synthesis of aurocyanide and auricyanide complexes of phosphines, phosphine sulfides and phosphine selenides, and their characterization by IR, far-IR, UV solution, and solid-state NMR spectroscopic methods

Bassem A. Al-Maythalony[a]; Mohamed I. M. Wazeer[a]; Anvarhusein A. Isab[a]
[a] Department of Chemistry, King Fahd University of Petroleum & Minerals, Dhahran 31261, Saudi Arabia

To cite this Article Al-Maythalony, Bassem A. , Wazeer, Mohamed I. M. and Isab, Anvarhusein A.(2010) 'Synthesis of aurocyanide and auricyanide complexes of phosphines, phosphine sulfides and phosphine selenides, and their characterization by IR, far-IR, UV solution, and solid-state NMR spectroscopic methods', Journal of Coordination Chemistry, 63: 21, 3824 — 3832

To link to this Article: DOI: 10.1080/00958972.2010.518759
URL: http://dx.doi.org/10.1080/00958972.2010.518759

Journal of Coordination Chemistry
Vol. 63, No. 21, 10 November 2010, 3824–3832

Taylor & Francis
Taylor & Francis Group

Synthesis of aurocyanide and auricyanide complexes of phosphines, phosphine sulfides and phosphine selenides, and their characterization by IR, far-IR, UV solution, and solid-state NMR spectroscopic methods

BASSEM A. AL-MAYTHALONY, MOHAMED I.M. WAZEER
and ANVARHUSEIN A. ISAB*

Department of Chemistry, King Fahd University of Petroleum & Minerals,
Dhahran 31261, Saudi Arabia

(*Received 8 April 2010; in final form 16 July 2010*)

A series of aurocyanide and auricyanide complexes of phosphines, phosphine sulfides, and phosphine selenides were synthesized. These new complexes have the general formula $[L_nAu(CN)_m]$, where L could be Cy_3P, $(2\text{-}CN\text{-}Et)_3P$, Me_3PS, Et_3PS, Ph_3PS, Me_3PSe, or Ph_3PSe. Auricyanide was reacted with L at 1 : 2 ratio. Products were characterized using elemental analysis, melting point, UV, IR, far-IR solution, and solid-state NMR spectroscopy. Phosphine ligands cause gold(III) reduction to gold(I); less redox tendency was found for phosphine sulfides and phosphine selenides. Tri-coordinate complexes $[L_2AuCN]$ were produced from phosphine ligands with gold-tetracyanide. IR and UV spectroscopic methods were used to identify gold oxidation state in the synthesized complexes.

Keywords: Solid state NMR; Solution NMR; IR; Far-IR; UV; Auricyanide; Phosphines; Phosphine sulfides; Phosphine selenides

1. Introduction

Gold complexes have been used in the treatment of rheumatoid arthritis for over seven decades [1–3], in what is called chrysotherapy [4]. The first-generation injectable drugs Solganal (gold thioglucose, AuSTg) and Myochrysine (gold sodium thiomalate, AuSTm) followed by the second-generation orally administered auranofin (2,3,4,6-tetra-O-acetyl-β-1-D-thioglucopyranosato-S-(triethylphosphine))gold(I), ($Et_3PAuSATg$) [5] have been developed. Both Solganal and auranofin bind to albumin by the exchange of its tetraacetyl thioglucose ligand by L-cysteine [6]. Despite being used for over 70 years for the treatment of rheumatoid arthritis, the anti-cancer potential of gold complexes has been suggested by Shaw only in 1999 [7].

Auricyanide complexes were considered as metabolism products of anti-arthritic gold(I) *in vivo* [5]. It was suggested that anti-rheumatic gold complexes are activated by their conversion to aurocyanide [8]. Tiekink [9] reported that gold(I) complexes are

---

*Corresponding author. Email: aisab@kfupm.edu.sa

Journal of Coordination Chemistry
ISSN 0095-8972 print/ISSN 1029-0389 online © 2010 Taylor & Francis
DOI: 10.1080/00958972.2010.518759

resilient *in vivo* in inflamed tissues; however, they may experience oxidative bursts, resulting in them being oxidized to gold(III). This stimulates the study of gold(III)-tetracyanide interaction with various biologically important ligands.

Notable results for the anti-tumor applications of gold(III) complexes have been reported, which showed promising cytotoxic properties toward cancer cells, both *in vitro* and *in vivo* [10]. Several multidentate ligands were used to build square planar gold(III) complexes [11, 12]. The importance of phosphine ligands in gold chemistry comes from their use in anti-rheumatic drugs (e.g., auranofin) and from reports about anti-cancer activity of gold–phosphine complexes [13].

In this study, we report the synthesis and characterization of new aurocyanide and auricyanide complexes with several phosphines, phosphine sulfides, and phosphine selenides.

2. Experimental

2.1. *Preparation of* $K[Au(CN)_4]$

Gold(III)-tetracyanide was prepared according to the literature [5]. Two solutions were prepared separately; solution A consists of 2.00 g (5.33 mmol) auric acid dissolved in 5 mL distilled water, and solution B, 1.73 g KCN (8% $K^{13}C^{15}N$ enriched; 26.62 mmol) dissolved in 5 mL distilled water. Solutions A and B were mixed while stirring (this reaction was done in a fume hood, to avoid the harmful effect of the production of HCN gas); a white precipitate was formed immediately, and when allowed to stand for 3 h, produced a solid, which was separated by decantation and dried in air; 95% yield was obtained. IR data showed $\nu_{(CN^-)}$ at 2189 cm^{-1}, corresponding to $[Au(CN)_4]^-$ that agreed with the literature [5].

2.2. $K[Au(CN)_4]$ *reaction with phosphines*

$K[Au(CN)_4]$ (~0.6 mmol) was dissolved in 15 mL acetone. Ligand (~1.2 mmol) was dissolved in 20 mL absolute ethanol; the two solutions were mixed in a round bottom flask, refluxed for ~3 h at 75°C, and the resulting solution was filtered and concentrated. Complexes were dried and the yields were ~30% for $[((2\text{-CN-Et})_3P)_2AuCN]$ and $K[(Cy_3P)_2Au(CN)_2]$, while general yields for the other complexes were in the range 25–55%. Crystals with twining were obtained for some complexes; however, when recrystallized in other solvents gold(III), they were reduced to gold(I); so no X-ray results were possible. Elemental analysis and melting point data for the synthesized complexes are given in table 1.

2.3. *IR and far-IR studies*

The solid-state IR spectra of the ligands and their gold(III) complexes were recorded on a Perkin-Elmer FTIR 180 spectrophotometer using KBr pellets from 4000 to 400 cm^{-1}. Far-IR spectra were recorded at 2 cm^{-1} resolution at room temperature using cesium chloride discs on a Nicolet 6700 FT-IR with far-IR beam splitter.

Table 1. Data from elemental analysis and melting points of the complexes.

		Found (Calcd) %			
Complex	m.p. (°C)	C	H	N	S
$[((2\text{-CN-Et})_3P)_2AuCN]$	205–206	38.65(38.44)	4.05(3.97)	15.91(16.09)	–
$K[(Cy_3P)_2Au(CN)_2]$	137–138	53.87(53.76)	7.55(7.84)	3.45(3.30)	–
$[(Me_3PS)_2Au(CN)_3]$	Decomposed	22.56(22.00)	3.70(3.69)	8.87(8.55)	12.59(13.05)
$[(Et_3PS)_3Au(CN)_3]$	94–96	34.19(34.76)	6.30(6.25)	5.61(5.79)	13.14(13.25)
$[(Ph_3PS)_2Au(CN)_3]$	160–161	54.65(54.23)	3.65(3.51)	4.62(4.87)	7.23(7.42)
$[(Me_3PSe)_2Au(CN)_3]$	150–152	18.14(18.47)	3.09(3.11)	6.97(7.18)	–
$[(Ph_3PSe)Au(CN)_3] \cdot KCN$	181–183	38.06(38.77)	2.20(2.22)	8.03(8.22)	–

2.4. *NMR measurements*

All NMR measurements were carried out on a JEOL JNM-LA 500 NMR spectrophotometer at 297 K using 0.10 mol L^{-1} solution of the complexes in CD_3OD. ^{13}C-NMR spectra were obtained at 125.65 MHz with ^{1}H broadband decoupling. ^{31}P-NMR spectra were obtained at 101.3 MHz; the chemical shifts are reported using trimethylphosphate (TMP; $\delta = 2.74$ ppm relative to external 85% H_3PO_4) as an external standard. The spectral conditions were: 32 K data points, 0.967 s acquisition time, 1.00 s pulse delay, and 45° pulse angle.

2.5. *Solid state NMR spectroscopy*

The $^{13}C\{^1H\}$ solid-state NMR spectra were obtained on a JEOL LAMBDA 500 spectrometer operating at 125.65 MHz (11.74 T), at 25°C. Samples were packed into 6 mm zirconium oxide rotors. Cross-polarization and high-power decoupling were employed. Pulse delay of 7.0 s and a contact time of 5.0 ms were used in the cross-polarization magic-angle spinning (CPMAS) experiments. The magic angle spinning rates were from 2 to 4 kHz. Carbon chemical shifts were referenced to TMS by setting the high-frequency isotropic peak of solid adamantane to 38.56 ppm. Solid-state CPMAS $^{31}P\{^1H\}$ NMR spectra were obtained at ambient temperature on the same spectrometer, operating at a frequency of 202.35 MHz. A contact time of 3 ms was used with a proton pulse width of 6 μs, with a recycle delay of 10 s. Chemical shifts were referenced using an external sample of solid PPh_3 ($\delta = 8.40$ ppm from 85% H_3PO_4).

Both ^{31}P and ^{13}C spectra, containing spinning side-band manifolds, were analyzed using a program HBA [14] based on Maricq and Waugh [15], which was developed at Dalhousie University, Canada, and University of Tübingen, Germany. The ^{13}C and ^{31}P solid-state NMR data are given in tables 2 and 3, respectively.

3. Results

All reactions were carried out by mixing $K[Au(CN)_4]$ with L at 1 : 2 ratio. Data on chemical formula, melting points, and elemental analysis are given in table 1. IR and

Table 2. Solid-state ^{13}C, isotropic chemical shifts (δ_{iso}) and principle shielding tensors (σ_{xx}) of cyanide in gold(III)–tetracyanide complexes with phosphine ligands.

Complex	δ_{iso}[a]	σ_{11}	σ_{22}	σ_{33}	Span (Ω)[b]	Skew (κ)[c]
$K[Au(CN)_4]$	110.0	236	138	−46	282	0.30
$(2\text{-}CN\text{-}Et)_3P$	122.9	231	207	−70	302	0.84
$[((2\text{-}CN\text{-}Et)_3P)_2AuCN]$	(i) 127.1	216	124	41	175	−0.05
	(ii) 123.7	266	193	−88	354	0.59
$[(Me_3PS)_2Au(CN)_3]$	105.3	222	123	−29	250	0.22
$[(Ph_3PS)_2Au(CN)_3]$	128.5	220	149	17	203	0.30
$[Ph_3PSeAu(CNw)_3]\cdot KCN$	125.2	204	142	30	173	0.28

[a] $\delta_{iso} = (\sigma_{11} + \sigma_{22} + \sigma_{33})/3$.
[b] Span $(\Omega) = \sigma_{33} - \sigma_{11.}$
[c] Skew $(\kappa) = 3(\sigma_{22} - \delta_{iso})/\Omega$ [14–17].

Table 3. Solid-state ^{31}P-NMR, isotropic chemical shifts (δ_{iso}) and principle shielding tensors (σ_{xx}) of gold(III)–tetracyanide complexes with phosphine ligands.

Compound	δ_{iso}[a]	σ_{11}	σ_{22}	σ_{33}	Span (Ω)[b]	Skew (κ)[c]
$(2\text{-}CN\text{-}Et)_3P$	−32.2	−15	−41	−41	26	−1.00
$[((2\text{-}CN\text{-}Et)_3P)_2AuCN]$	49.5	130	82	−63	193	0.50
$K[(Cy_3P)_2Au(CN)_2]$	50.3	112	98	−59	171	0.83
Et_3PS	59.7	109	96	−25	134	0.80
$[(Et_3PS)_3Au(CN)_3]$	59.8	107	97	−25	131	0.85
Ph_3PS	45.3	112	80	−56	167	0.62
$[(Ph_3PS)_2Au(CN)_3]$	45.4	107	86	−56	163	0.75
Ph_3PSe	36.8	111	51	−52	163	0.27
$[Ph_3PSeAu(CN)_3]\cdot KCN$	36.8	96	60	−46	143	0.50

[a] $\delta_{iso} = (\sigma_{11} + \sigma_{22} + \sigma_{33})/3$.
[b] Span $(\Omega) = \sigma_{33} - \sigma_{11.}$
[c] Skew $(\kappa) = 3(\sigma_{22} - \delta_{iso})/\Omega$ [14–19].

Table 4. Solid (KBr-disc) IR and (CsCl-disc) far-IR data of the complexes.

Complex	$\nu_{(C\equiv N)}$ (cm^{-1})	$\nu_{(Au–C)}$ (cm^{-1})	$\upsilon_{(P–S/P–Se)}$ (cm^{-1})	$\upsilon_{(P–S–Au/P–Se–Au)}$ (cm^{-1})
$K[Au(CN)_2]$	2140	471[a]	–	–
$K[Au(CN)_4]$	2189	418	–	–
$[((2\text{-}CN\text{-}Et)_3P)_2AuCN]$	2245, 2240, 2136	437	–	–
$K[(Cy_3P)_2Au(CN)_2]$	2140	419	–	–
$[(Me_3PS)_2Au(CN)_3]$	2186, 2171, 2148	413	565	557
$[(Et_3PS)_3Au(CN)_3]$	2186, 2144, 2064	419	537	536
$[(Ph_3PS)_2Au(CN)_3]$	2192	410	540	516
$[(Me_3PSe)_2Au(CN)_3]$	2179, 2144, 2066	411	562	516
$[(Ph_3PSe)Au(CN)_3]\cdot KCN$	2189, 2143, 2105	419	562	561

[a] As reported by Bowmaker *et al.* [20].

UV spectra were measured for the complexes. All gold(III) complexes showed at least one IR band corresponding to cyanide in the range 2179–2192 cm^{-1}, which was missing for gold(I) complexes. IR bands, corresponding to CN, characteristic for each compound are mentioned below, while other frequencies are included in table 4.

3.1. $[((2\text{-CN-Et})_3P)_2AuCN]$

IR spectrum shows CN stretching bands at 2245 and 2240 cm^{-1} corresponding to cyanide stretching in (2-CN-Et)$_3$P, and the other band at 2136 cm^{-1} corresponding to CN attached to gold, as reported earlier by Yangyuoru *et al.* [5], which is characteristic of Au(I)–cyanide. UV spectrum shows absorption bands at 204–240 nm, characteristic for Au(I)–cyanide [5].

3.2. $K[(Cy_3P)_2Au(CN)_2]$

IR spectrum shows a band at 2140 cm^{-1} that is characteristic for Au(I)–CN [21]. Band corresponding to unbound cyanide could not be detected; therefore, a tetra-coordinate structure was suggested for this complex. UV absorption spectrum shows absorption bands at 204–240 nm corresponding to Au(I)–CN [5].

3.3. $[(Me_3PS)_2Au(CN)_3]$

IR data show three stretching frequencies for cyanide including 2186 cm^{-1} that is characteristic for Au(III)–CN; no distinct signals were found in UV.

3.4. $[(Et_3PS)_3Au(CN)_3]$

IR vibration spectrum shows a band at 2186 cm^{-1} assigned to Au(III)–CN, and no distinct signals in UV.

3.5. $[(Ph_3PS)_2Au(CN)_3]$

IR spectrum showed cyanide stretching frequency at 2192 cm^{-1} characteristic of Au(III)–CN, and no distinct signals in UV.

3.6. $[(Me_3PSe)_2Au(CN)_3]$

IR data show CN stretch at 2179 cm^{-1}, characteristic of Au(III)–CN, and no distinct signals were found in UV corresponding to Au(I)–CN.

3.7. $[(Ph_3PSe)Au(CN)_3]\cdot KCN$

IR data show a CN stretch at 2189 cm^{-1} characteristic of CN bound to Au(III) as shown by Yangyuoru *et al.* [5].

4. Discussion

Phosphine reaction with $[Au(CN)_4]^-$ results in the formation of tri-coordinate complexes, common in the literature, as reported for $[Au(PPh_3)_2Cl]$ complexes by Parish [22] and Tiekink *et al.* [23].

Table 4 shows IR and far-IR data of the synthesized complexes. $K[Au(CN)_4]$ showed a stretching band at 2189 cm^{-1} that corresponds to stretching band of cyanide in Au(III)–CN [5], while the IR spectrum of $K[Au(CN)_2]$ shows the stretch at 2140 cm^{-1} [21, 24, 25]. The difference in cyanide IR stretching bands results from higher electron density at gold(I) leading to more π-back donation to cyanide, increasing the electron density in the cyanide anti-bonding orbital (π^*) and weakening of the C–N bond. Fewer coordinating ligands in $K[Au(CN)_2]$ will also increase the electron back donation from metal to ligand; so Au–C gets shorter and C≡N longer; this is consistent with the IR and far-IR bands for $K[Au(CN)_2]$. The reverse is true for $K[Au(CN)_4]$.

Signals corresponding to cyanide in IR and UV could be employed for characterization of gold oxidation state; cyanide in gold(III) complexes shows at least one stretching band in the range 2192–2186 cm^{-1}, while this band is absent in all gold(I) complexes. The cyanide signal in gold(I) complexes is at 2142–2136 cm^{-1}, and UV spectroscopy shows four absorption bands at 204–240 nm in UV spectrum, as shown by Yangyuoru *et al.* [5]. This band can also be used as an indication of the gold oxidation state in complexes, as these bands were absent in UV of gold(III) complexes.

Far-IR of phosphine complexes must be interpreted with caution because of the bending vibrations of phenyl-P-phenyl that absorb at less than 550 cm^{-1} [26]. Far-IR data of $K[Au(CN)_4]$ show Au–C vibration at 418 cm^{-1}, while 471 cm^{-1} was observed for $K[Au(CN)_2]$ [20]. Difference in stretching bands between the two complexes is due to stronger Au–C bond in Au(I) complex causing the shift to higher wavenumber, while longer Au–C bond is expected for Au(III) complexes that result in a red shift. This interpretation is consistent with the experimental results. This also could be used as a criterion to distinguish gold oxidation states in complexes. Table 4 shows a blue shift of the Au–C stretching band in gold(I) complexes while red shift for gold(III) complexes.

IR stretches of P–S and P–Se [27] show decrease in frequency upon complexation, due to electron donation from sulfur and selenium to the metal, enhancing π-back donation and leading to a higher level of electron density on the π^* orbital, weakening P–S and P–Se bonds after complexation.

^{13}C- and ^{31}P-NMR chemical shifts are given in table 5. ^{13}C-NMR chemical shift of cyanide in complexes was useful in identification of gold oxidation state. Canumalla *et al.* [28] reported that cyanide signal in Au(III)–CN complexes appeared at ~115 for *cis* and 120 for *trans* in D_2O for monosubstituted $[LAu(CN)_3]$ while at 125 ppm for $[L_2Au(CN)_2]^+$. Chemical shift for cyanide attached to gold(I) as $[Au(CN)_2]^-$ was reported to appear at 156 ppm in D_2O [28] and found at 152 ppm in CD_3OD in our study.

^{31}P-NMR shows clear downfield shift for phosphines in complexes while very small change in chemical shift was found when L represents phosphine sulfides or phosphine selenides.

When gold(III) complexes were heated overnight at 60°C and their ^{13}C-NMR recorded, $[Au(CN)_2]^-$ resonance at 152 ppm appeared indicating reduction of gold(III) to gold(I) complexes [18, 19].

Solid state ^{13}C-NMR data for the synthesized complexes are given in table 2. Cyanide isotropic signal shows downfield shift in the complex in comparison with $K[Au(CN)_4]$. In aryl-phosphine–gold complexes, cyanide ^{13}C-NMR signals overlap with aromatic

Table 5. ^{31}P- and ^{13}C-NMR chemical shifts of the complexes in CD_3OD at 25°C.

	L–Au–(CN), ^{13}C $\delta_{(C\equiv N)}$	L, ^{31}P δ	L–Au–(CN),^{31}P δ
KCN	163.60		
$KAu(CN)_2$	152.21		
$KAu(CN)_4$	103.47		
$[((2\text{-CN-Et})_3P)_2AuCN]$	120.17, 120.05	−32.21	49.36
$K[(Cy_3P)_2Au(CN)_2]$	113.04	58.51	61.33, 60.50
$[(Me_3PS)_2Au(CN)_3]$	–	33.68	33.75
$[(Et_3PS)_3Au(CN)_3]$	116.72	56.82	51.41
$[(Ph_3PS)_2Au(CN)_3]$	106.21	43.83	43.85
$[(Me_3PSe)_2Au(CN)_3]$	–	–	48.55
$[(Ph_3PSe)Au(CN)_3]\cdot KCN$	117.91	35.89	35.89

carbon spinning side manifold, which are more intense, because of the attached hydrogen to carbon, increasing the signal intensity in CPMAS experiments. Comparison of cyanide resonance by solid-state ^{13}C-NMR reveals downfield shift after reaction with phosphine ligands (table 2). The same results were found in solution and solid NMR. Another observation was the higher downfield shift by solid state NMR, because of solvent absence; so less shielded nuclei are expected in solid-state NMR.

Data of solid-state ^{31}P-NMR isotropic signals and tensors (σ_{xx}) are given in table 3. The isotropic signal of the complex shows obvious changes in chemical shift for phosphine complexes while minor change or no change was found for phosphine sulfides and phosphine selenides in which phosphorus is far from the binding site; another explanation for this could be the presence of p_π–d_π bond leading to increase in electron density around phosphorus, thus augmenting its shielding; similar result was concluded from solution NMR data [21]. It is interesting to note that the skew factor κ for the phosphine ligand changed from 1 (axial symmetry) to 0.5 (non-axial) on complexation.

Several complexes discussed in this study have unusual five and six coordination numbers, e.g., $[(Me_3PS)_2Au(CN)_3]$, $[(Et_3PS)_3Au(CN)_3]$, $[(Ph_3PS)_2Au(CN)_3]$, and $[(Me_3PSe)_2Au(CN)_3]$. Unusual coordination numbers of gold complexes have been discussed in several places mainly for Au(II) complexes [29–33]. Huang *et al.* [29] reported the structure of $[Au([9]aneS_2O)_2]^{2+}$, where $[9]aneS_2O$ refers to 1-oxa-4,7-dithiacyclononane. The O-donors in $[Au([9]aneS_2O)_2]^{2+}$ occupy axial positions about Au(II) [(Au $\cdots$ O) 2.718(2) Å] with the S-donors occupying the equatorial plane [Au-S 2.428(8) and 2.484(8) Å]. However, unusual coordination was also reported for Au(III) complexes. The $[Au([9]aneS_2O)_2]^{3+}$ complex was reported to have a coordination sphere similar to that of $[Au([9]aneS_2O)_2]^{2+}$ but with significantly shorter axial Au $\cdots$ O interactions [2.688(2) Å] and equatorial Au–S bond lengths [2.340(4) and 2.355(6) Å].

5. Conclusion

Gold(III)-tetracyanide was reacted with phosphine, phosphine sulfides, and phosphine selenides at 1 : 2 ratio. Phosphines react by cyanide exchange from $[Au(CN)_4]^-$, while oxidation of phosphine and reduction of gold(III) into gold(I) take place in some reactions. Products were characterized using elemental analysis, melting point method and IR, far-IR, UV solution, and solid-state NMR spectroscopic methods for ^{13}C and ^{31}P nuclei (tables 2–5). It was observed that phosphine ligands can cause gold(III) reduction into gold(I), while phosphine sulfide and phosphine selenide ligands react simply by exchange of cyanide. IR, far-IR, and UV spectroscopic methods can provide good and complementary data by which gold oxidation state can be characterized.

Acknowledgments

The authors acknowledge the support by the Deanship of Scientific Research at King Fahd University of Petroleum & Minerals for funding this study through project no. IN080421.

References

[1] S. Ahmad, A.A. Isab, S. Ali, A.R. Al-Arfaj. *Polyhedron*, **25**, 1633 (2006).
[2] A. Casini, C. Hartinger, C. Gabbiani, E. Mini, P.J. Dyson, B.K. Keppler, L. Messori. *J. Inorg. Biochem.*, **102**, 564 (2008).
[3] O. Ingo. *Coord. Chem. Rev.*, **253**, 1670 (2009).
[4] A.A. Isab, C.F. Shaw, A. Munoz, J.D. Hoesschele. *Inorg. React. Mech.*, **5**, 109 (2004).
[5] P.M. Yangyuoru, J.W. Webb, C.F. Shaw. *J. Inorg. Biochem.*, **102**, 584 (2008).
[6] O.M. Ni Dhubhghaill, P.J. Sadler, A. Tucker. *J. Am. Chem. Soc.*, **114**, 1118 (1992).
[7] C.F. Shaw. *Chem. Rev.*, **99**, 2589 (1999).
[8] G.G. Graham, A.J. Kettle. *Biochem. Pharmacol.*, **56**, 307 (1998).
[9] E.R.T. Tiekink. *Inflammopharmacology*, **16**, 138 (2008).
[10] S. Carotti, G. Marcon, M. Marussich, T. Mazzei, L. Messori, E. Mini, P. Orioli. *Chem. Biol. Interact.*, **125**, 29 (2000).
[11] U. Sampath, W.C. Putnam, T.A. Osiek, S. Touami, J. Xie, D. Cohen, A. Cagnolini, P. Droege, D. Klug, C.L. Barnes, A. Modak, J.K. Bashkin, S.S. Jurisson. *J. Chem. Soc., Dalton Trans.*, 2049 (1999).
[12] C.M. Che, R.W.Y. Sun, Z.F. Yang, C.K.L. Li, United States, Patent Application Publication (10th July 2008), Pub. no. US2008/0166429 A1.
[13] S.J. Berners-Price, R.J. Bowen, T.W. Hambley, P.C. Healy. *J. Chem. Soc., Dalton Trans.*, 1337 (1999).
[14] K. Eichele, R.E. Wasylischen. *WSolid1 NMR Simulation Package (Version 1.4.4)*, Dalhousie University, Canada and University of Tübingen, Germany (2001).
[15] M. Maricq, J. Waugh. *J. Chem. Soc.*, **70**, 3300 (1979).
[16] N.D. Draper, R.J. Batchelor, P.M. Aguiar, S. Kroeker, D.B. Leznoff. *Inorg. Chem.*, **43**, 6557 (2004).
[17] M. Fettouhi, M.I.M. Wazeer, A.A. Isab. *Inorg. Chem. Commun.*, **11**, 252 (2008).
[18] V.P. Dyadchenko. *Russ. Chem. Rev.*, **51**, 265 (1982).
[19] (a) C. Kowala, J.M. Swan. *Aust. J. Chem.*, **19**, 547 (1966); (b) D.T. Hill, B.M. Sutton, A.A. Isab, T. Razi, P.J. Sadler, J.M. Trooster, G.H.M. Calis. *Inorg. Chem.*, **22**, 2936 (1983).
[20] G.A. Bowmaker, B.J. Kennedy, J.C. Reid. *Inorg. Chem.*, **37**, 3968 (1998).
[21] S. Ahmad, A.A. Isab, H.P. Perzanowski, M.S. Hussain, M.N. Akhtar. *Transition Met. Chem.*, **27**, 177 (2002).
[22] R.V. Parish. *Gold Bull.*, **15**, 51 (1982).
[23] E.R.T. Tiekink, J.G. Kang. *Coord. Chem. Rev.*, **253**, 1627 (2009).
[24] L.H. Jones. *J. Chem. Phys.*, **27**, 468 (1957).
[25] M.H. Ford-Smith, J.J. Habeeb, J.H. Rawsthorne. *J. Chem. Soc., Dalton Trans.*, 2116 (1972).
[26] K. Shobatake, C. Postmus, J.R. Ferraro, K. Nakamoto. *Appl. Spectrosc.*, **23**, 12 (1969).
[27] J.R. Durig, J.S. Di Yorio, D.W. Wertz. *J. Mol. Spectrosc.*, **28**, 444 (1968).
[28] A.J. Canumalla, N. Al-Zamil, M. Philips, A.A. Isab, C.F. Shaw III. *J. Inorg. Biochem.*, **85**, 67 (2001).

[29] D. Huang, X. Zhang, E.J.L. McInnes, J. McMaster, A.J. Blake, E.S. Davies, J. Wolowska, C. Wilson, M. Schröder. *Inorg. Chem.*, **47**, 9919 (2008).
[30] M.C. Gimeno, A. Laguna. *Gold Bull.*, **36**, 83 (2003).
[31] M.C. Gimeno, A. Laguna. *Chem. Rev.*, **97**, 511 (1997).
[32] H.E. Abdou, A.A. Mohamed, J.P. Fackler. *Gold(I) Nitrogen Chemistry*. *Gold Chemistry*, pp. 1–45, Wiley-VCH Verlag GmbH & Co. KGaA (2009). ISBN: 978-3-527-32086-8.
[33] M.A. Bennett, S.K. Bhargava, N. Mirzadeh, S.H. Privèr, J. Wagler, A.C. Willis. *Dalton Trans.*, 7537 (2009).